Progress on the Micro-X rocket payload

Progress on the Micro-X Rocket Payload

E. Figueroa-Feliciano[a,b], P. Wikus[b], J. S. Adams[c,d], S. R. Bandler[c,d], M. Bautz[b], K. Boyce[c], G. Brown[e], S. Deiker[f], W. B. Doriese[g], K. Flanagan[b], M. Galeazzi[h], G. C. Hilton[g], U. Hwang[c], K. D. Irwin[g], T. Kallman[c], R. L. Kelley[c], C. A. Kilbourne[c], S. Kissel[b], S. W. Leman[b], A. Levine[b], M. Loewenstein[c,d], D. Martinez-Galarce[f], D. McCammon[i], R. Mushotzky[c], R. Petre[c], F. S. Porter[c], C. D. Reintsema[g], J. M. Rutherford[a], T. Saab[j], P. Serlemitsos[c], N. Schulz[b], R. Smith[c], J. N. Ullom[g]

[a]Department of Physics, Massachusetts Institute of Technology, Cambridge, MA 02139, USA;
[b]MIT Kavli Institute for Astrophysics and Space Research, Cambridge, MA 02139, USA;
[c]NASA Goddard Space Flight Center, Greenbelt, MD 20770, USA;
[d]University of Maryland, Department of Astronomy, College Park, MD 20742, USA;
[e]High Energy Density Physics and Astrophysics Division, Lawrence Livermore National Laboratory, Livermore, CA 94550;
[f]Lockheed Martin Solar and Astrophysics Laboratory, 3176 Porter Dr., Palo Alto, CA 94304;
[g]National Institute of Standards and Technology, 325 Broadway, Boulder, CO 80305, USA;
[h]University of Miami, Department of Physics, Coral Gables, FL 33146, USA;
[i]Department of Physics, University of Wisconsin-Madison, Madison, WI 53706, USA;
[j]Department of Physics, University of Florida, Gainesville, FL 32611, USA

ABSTRACT

The Micro-X High Resolution Microcalorimeter X-ray Imaging Rocket is a sounding rocket experiment that will combine a transition-edge-sensor x-ray-microcalorimeter array with a conical imaging mirror to obtain high-spectral-resolution images of extended and point x-ray sources. The target for Micro-X's first flight (slated for January 2011) is the Puppis A supernova remnant. The Micro-X observation of the bright eastern knot of Puppis A will obtain a line-dominated spectrum with up to 90,000 counts collected in 300 seconds at 2 eV resolution across the 0.3-2.5 keV band. Micro-X will utilize plasma diagnostics to determine the thermodynamic and ionization state of the plasma, to search for line shifts and broadening associated with dynamical processes, and seek evidence of ejecta enhancement. We describe the progress made in developing this payload, including the detector, cryogenics, and electronics assemblies. A detailed modeling effort has been undertaken to design a rocket-bourne adiabatic demagnetization refrigerator with sufficient magnetic shielding to allow stable operation of transition edge sensors, and the associated rocket electronics have been prototyped and tested.

Keywords: Supernova Remnants, Puppis A, X-ray, Transition Edge Sensor, Microcalorimeter, Sounding Rockets

1. INTRODUCTION

The Micro-X High Resolution Microcalorimeter X-ray Imaging Rocket was selected by NASA as a sounding rocket mission to be launched in 2011 and will be the first space flight of a Transition Edge Sensor (TES) microcalorimeter array. The microcalorimeter is placed at the focus of a flight-proven conical x-ray imaging mirror, and will thus also obtain the first focused x-ray observation of an astrophysical source with a microcalorimeter.

Micro-X will offer a unique combination of bandpass, collecting area, and spectral and angular resolution. The spectral resolution across the 0.3-2.0 keV band will be 2 eV. The angular resolution across the 14.4 arc minute field of view will be 2.5 arc minutes. The effective area, 200 cm^2 at 1 keV, is sufficient to provide observations of unprecedented quality of numerous cosmic x-ray sources, discrete and extended, even in a brief sounding rocket exposure. Table 1 summarizes the technical specifications of Micro-X.

E. Figueroa-Feliciano's e-mail: enectali@mit.edu

Space Telescopes and Instrumentation 2008: Ultraviolet to Gamma Ray, edited by Martin J. L. Turner, Kathryn A. Flanagan, Proc. of SPIE Vol. 7011, 70113U, (2008) · 0277-786X/08/$18 · doi: 10.1117/12.789904

Table 1. Micro-X Technical Specifications

Energy Resolution ΔE	2	eV FWHM
Effective Area @ 1 keV	200	cm^2
Point Spread Function	2.5	arcmin
Mirror Focal Length	2.1	m
FOV	14.4	arcmin
Size of Detector Array	11×11	
Pixel Size	800	μm
	1.3	arcmin
Bandpass	0.3-2.5	keV

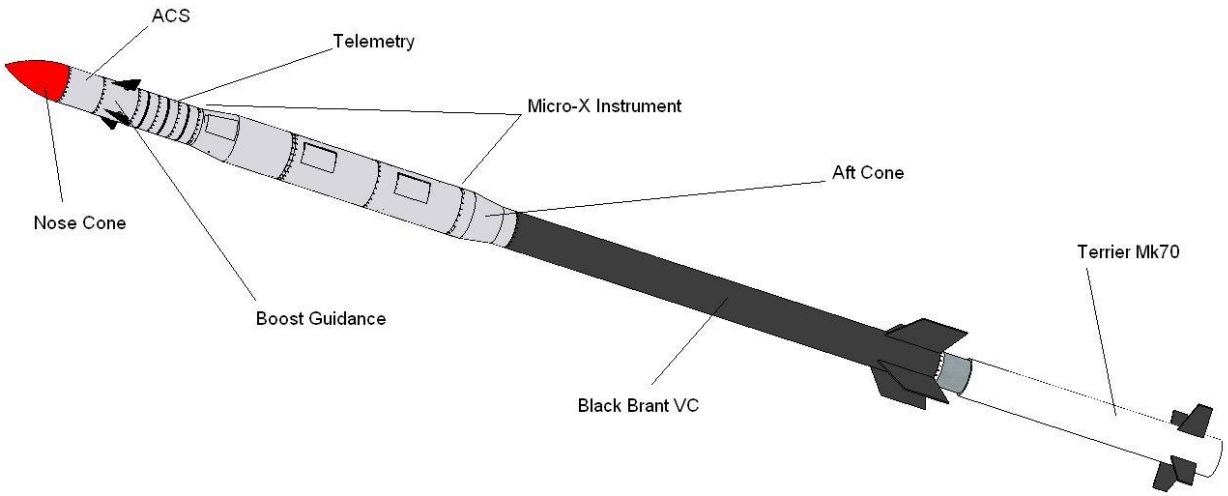

Figure 1. The Micro-X sounding rocket.

Our scientific program will initially focus on extended sources, for which high-spectral-resolution, wide-energy-bandwith observations were hitherto impossible. For our initial flight, we will observe the bright eastern knot (BEK) in the Puppis A remnant, a site of complex cloud-shock interactions and ejecta enrichment.

2. THE MICRO-X PAYLOAD

In this section we give a brief overview of the Micro-X sounding rocket instrument, which will be launched by a Black Brant sounding rocket. The payload of the rocket consists of the Micro-X instrument and several support systems, such as boost guidance, telemetry and attitude control. The Micro-X instrument has a mass of approximately 165 kg and a length of 3.5 m. It is accommodated inside a 22 inch rocket skin. Since the Black Brant motor and the standardized support systems have a diameter of 17.26 inches, conical adapters will be used. The Micro-X sounding rocket is shown in Figure 1.

The Micro-X instrument is located at the aft end of the payload, and attaches directly to the rocket motor, which is jettisoned after powered flight. Then, the shutter door opens and exposes the telescope, which peeks out through the instrument's aft end. A mirror projects the x-rays onto the microcalorimeter array which is located inside an adiabatic demagnetization refrigerator (ADR) near the front end of the instrument. The optical bench, a very rigid aluminum structure, aligns the mirror with respect to the ADR. The electronics controlling the cryogenic system and the data read out are accommodated in the avionics section above the ADR. A schematic of the instrument is shown in Figure 2.

In the following, we give a brief description of the most important subsystems:

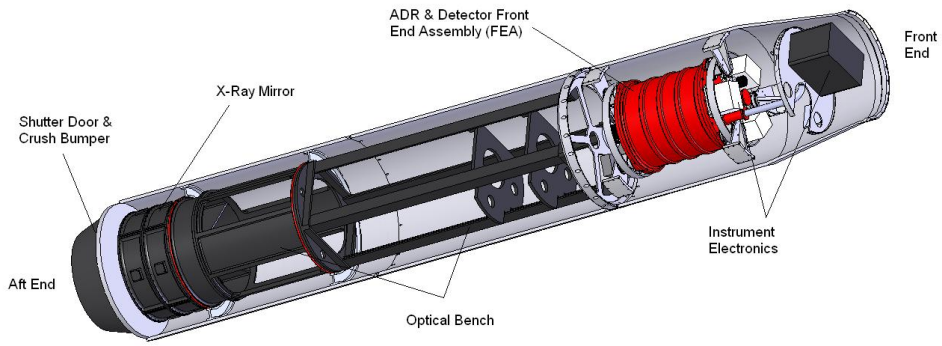

Figure 2. The Micro-X instrument.

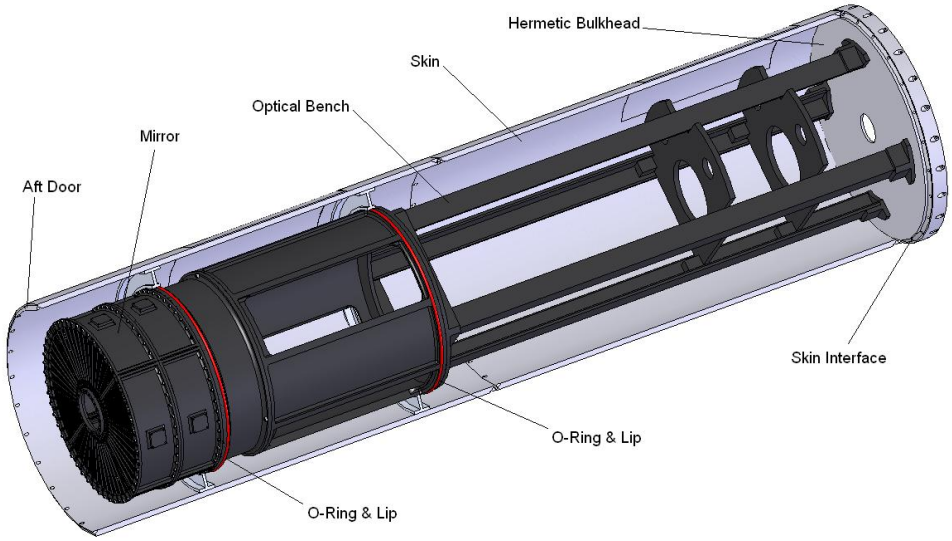

Figure 3. The Micro-X mirror and optical bench inside the rocket skin.

2.1. Mirror and optical bench

The Micro-X instrument uses the imaging mirror and optical bench from the Supernova X-Ray Spectrometer (SXS), a sounding rocket instrument flown by the GSFC group in 1988 to observe SN 1987A (Figure 3). The mirror is the first segmented, thin foil conical mirror ever to have flown. The foil reflectors were lacquer coated using the approach used for the BBXRT and ASCA mirrors. It has a 2.1 m focal length and a 40 cm diameter with 70 nested shells configured in quadrants. A ST5000 star tracker is located in the center bore of the mirror. The star tracker ensures accurate pointing of the instrument to within $\pm$ 0.5 arcmin.

The high filling factor of the thin-foil implementation provides > 300 cm^2 of area at 1 keV and a broad energy response. After including filter transmission and detector fill fraction we still have > 200 cm^2 of effective area (Figure 4). The optic's measured angular resolution is $\sim 2.5'$ (half power diameter).

2.2. Adiabatic Demagnetization Refrigerator (ADR)

The Micro-X ADR houses the microcalorimeter array and provides a heat sink for the detectors at the required temperature of 50 mK. Its design is based on the very successful X-ray Quantum Calorimeter (XQC) sounding rocket ADR.[1,2] Cooling is achieved by adiabatic demagnetization of 75 g of ferric ammonium alum (FAA) salt. At the projected heat load of 1 μW, and a starting temperature of 1.8 K, we expect a hold time at 50 mK of

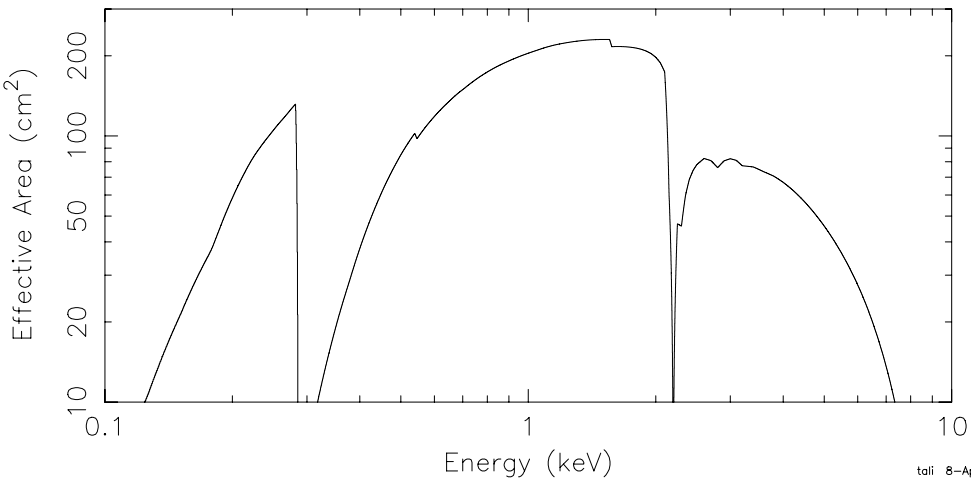

Figure 4. The Micro-X effective area, including the mirror, the blocking filters, and the TES quantum efficiency and packing fraction.

approximately 12 hours. The geometry of the magnet coil was optimized such that the maximum hold time for a given magnet mass is achieved.

Magnetic shielding had to be taken into account in this optimization process. TES detectors and SQUID readout systems are highly susceptible to magnetic fields. As a consequence, near-zero magnetic field regions are required in the instrument around the microcalorimeter front end assembly (FEA) and the SQUID amplifiers. We have designed a staged magnetic isolation system for the detectors and amplifiers. A bucking coil is located between the magnet and the FEA and reduces the field strength in the FEA region. In addition, the FEA is surrounded by a superconducting niobium shield. We are currently setting up a laboratory system to evaluate and optimize this magnetic shield design. If necessary, the magnetic shield can be further improved by adding a high permeability casing around the magnet.

In order to minimize the heat load on the ADR's cold stage, a suspension system featuring very low thermal conductivity has to be devised. At the same time, the suspension system must be sufficiently strong to withstand the launch loads of 20 g and the landing impact shock in excess of 100 g. Furthermore, the suspension system must be sufficiently rigid to raise the lowest resonance frequency of the support to several hundred Hz. This is necessary to allow for the implementation of a vibration isolation system featuring several stages with staggered resonance frequencies, which is required to minimize the heat input into the salt pill due to vibrations during powered flight. We have performed cryogenic tests on high-strength polyurethane fibers to assess their suitability for this application. Aramid fibers (such as Kevlar*, for instance) have also been used successfully for similar applications in the past.[3]

We expect to conduct first cryogenic performance tests on a prototype of the flight ADR by the end of this year.

2.3. Detectors and Readout Electronics

The Micro-X detector array consists of an 11×11 array of 0.7 mm $\times$ 0.7 mm pixels on an 0.8 mm pitch. This creates a "waffle-like" focal plane with dead region at the wiring gap between pixels. The 77% fill factor is adequate for our observations. Coupled to the 2.1 m focal length mirror, each array pixel will be 1.31 arcmin on the sky, a good match to the 2.5 arcmin imaging of the mirror. X-ray interaction in the electrical leads and silicon structure are prevented by a mask. The Micro-X microcalorimeters will be fabricated by the NASA Goddard Space Flight Center's X-ray Microcalorimeter Group (who have recently shown sub–2 eV resolution in devices with the bandpass for Micro-X[4]), and will have a energy resolution of 2 eV across the 0.3–2.5 keV bandpass.

*Kevlar is a registered trademark of DuPont Advanced Fibers Systems, Richmond, VA (USA).

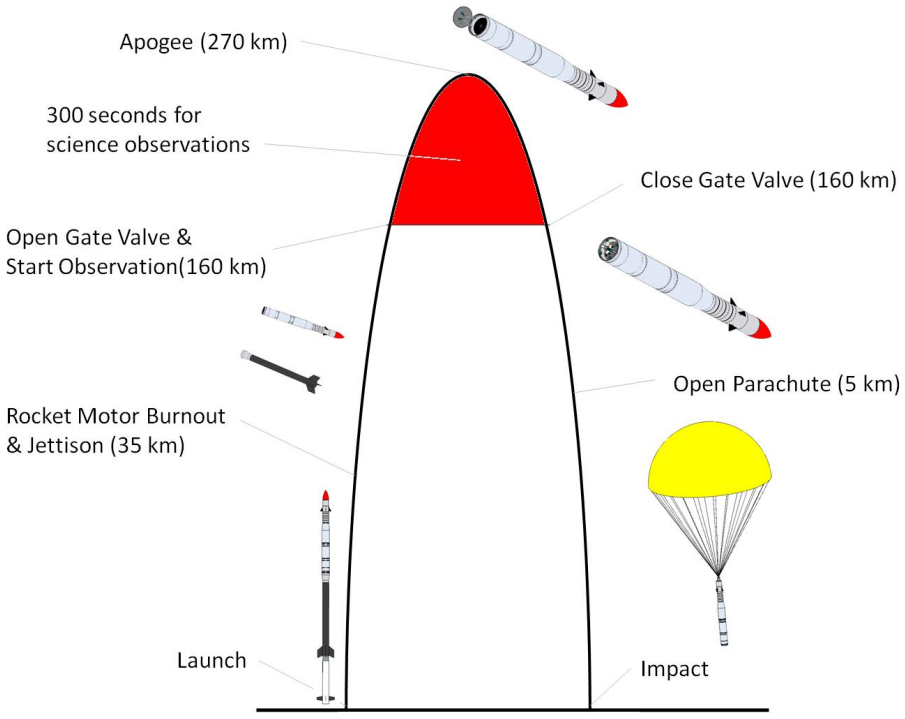

Figure 5. The Micro-X flight profile.

The detector will be read out with a time-division SQUID multiplexer. In a time-division multiplexer, amplifiers are turned on one at a time, with switching occurring fast enough that each detector is sampled faster than the detector time constants of interest. This system is described in a companion paper by Reintsema et al.[5] Micro-X will make use of two such multiplexing systems, each one reading out one half of the detector array. In case a malfunction should occur in one of the read-out systems, Micro-X will still return valuable science data.

3. MICRO-X FLIGHT TIMELINE

Our goal for the Micro-X flight is to obtain a minimum of 300 seconds worth of science data above an altitude of 160 km. As there is not sufficient time to cool the detectors to their operating temperature during the flight, the ADR has to be cycled on the launch rail, approximately one hour before lift off. After launch and before science observations can begin, the temperature control system has to return the cold stage temperature to its setpoint within only a few seconds after the rocket motors have burned out. While the temperature settles, the attitude control systems (ACS) aligns the rocket with the science target. A shutter door, which is located at the aft end of the Micro-X payload just in front of the x-ray mirror, is opened.

After tight temperature and attitude control have been achieved, a gate valve in the ADR's vacuum vessel is opened, and x-rays from the science target hit the detector array. First, we point Micro-X at a bright source in the sky and observe it for a few seconds. This is to verify the correct alignment between the star tracker and the telescope optics. If a misalignment is detected, we will command the ACS to point at a slightly offset point in the sky to compensate for that misalignment. Then, the instrument is pointed at Puppis A. As an alternative to this procedure (which may take a long as 100 sec), we are simulating the observation to determine if the Bright Eastern Knot of Puppis A itself can serve as the target for the optical alignment check. The science data of about half the pixels is sent to the ground via telemetry at a rate of 20 MBit/s. The entire data stream is stored on flash memory inside the rocket.

At an altitude of approximately 270 km, the rocket payload reaches its apogee and starts falling back to earth. At an altitude of some 160 km, science data taking ends, but we continue to take calibration data from

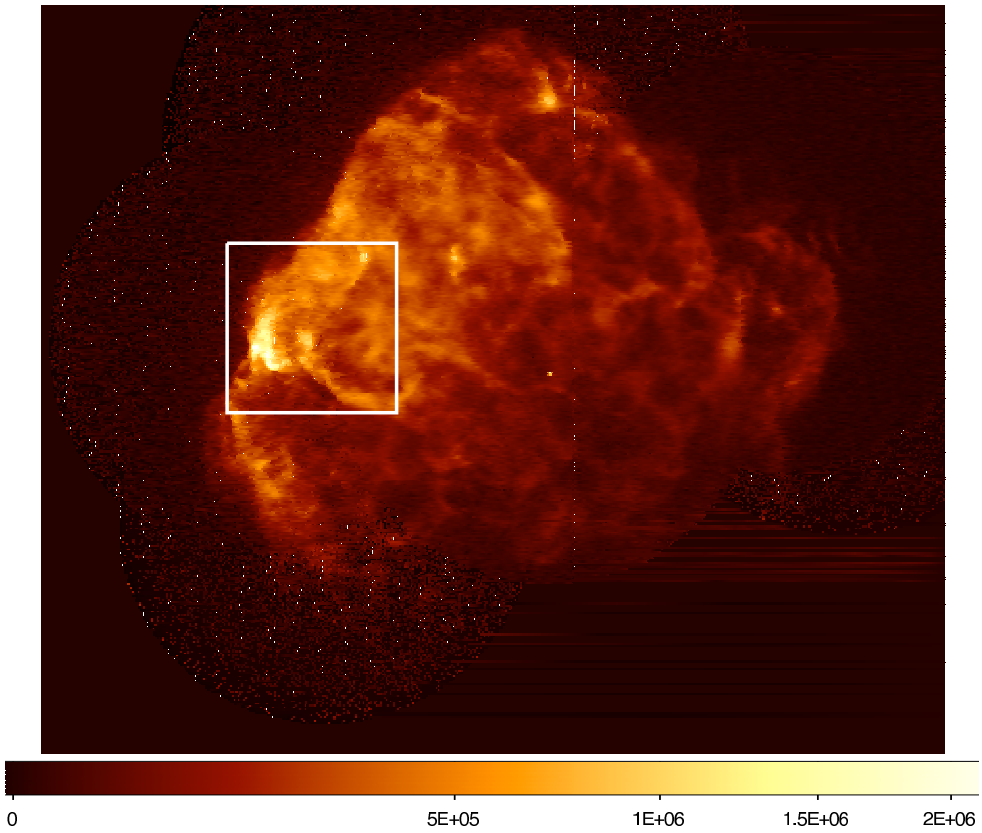

Figure 6. The Puppis A supernova remnant. The box represents the 14.4′ FOV for observation of the Bright Eastern Knot by Micro-X.

an x-ray source which is mounted inside the ADR. The gate valve and the shutter door are closed to protect the instrument during reentry. At an altitude of 5 km, the parachute opens. The payload is recovered along with post-flight calibration data.

4. THE PUPPIS A OBSERVATION WITH MICRO-X

The target for the first Micro-X observation is the Bright Eastern Knot region of the Puppis A supernova remnant (Figure 6). Other possible targets for subsequent flights are discussed elsewhere.[6] Puppis A is a bright galactic supernova remnant that was the target of one of the earliest successful high-resolution spectral observations with the Einstein Focal Plane Crystal Spectrometer.[7,8] These observations were of limited energy range and sensitivity, however, and the spectral resolution of this dispersive instrument was compromised by the large angular scale of the x-ray emission.

As a middle-aged remnant, Puppis A straddles the division between young objects that are totally dominated by their supernova debris, or ejecta, and older remnants that have lost all trace of their ejecta. Despite a rather advanced estimated age of 4000 years, it contains both optical and x-ray evidence for supernova ejecta. However, it is also very strongly shaped by its interactions with a complex interstellar environment. The Bright Eastern Knot (BEK) region of Puppis A is the brightest, and perhaps most complex example of these interactions, with multiple shocked clouds plus evidence for ejecta enrichment in its vicinity.

The main science goals of the Micro-X observation are first to unravel the kinematic, temperature, and ionization characteristics of the cloud-shock interactions at the BEK, and second to address the issue of ejecta enrichment of the x-ray emitting gas. Crucial to both of these efforts will be ascertaining the temperature

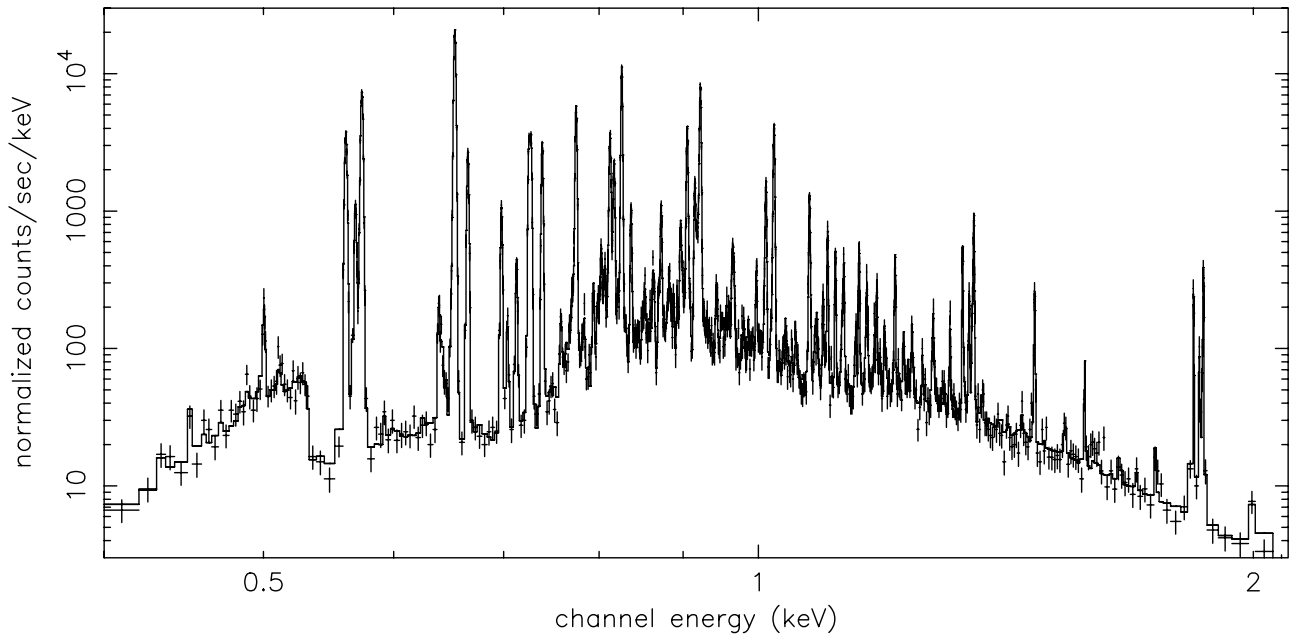

Figure 7. Simulation of the integrated Puppis A spectrum assuming 300 sec observation by Micro-X with 2 eV resolution. There are 92,900 counts in this simulation. The effective area curve used for this simulation, which includes mirror, filters, and detector efficiencies is shown in Figure 4.

distribution of the x-ray emitting gas. This is important for understanding ejecta enrichment because multi-temperature gas can mimic enriched abundances in lower resolution spectra if too simple a temperature structure is assumed. A simulated 300 s observation with a 14.4 arcmin field of view at the BEK is shown in Figure 7. The model in Figure 7 is a three-temperature nonequilibrium ionization thermal model that approximates the integrated spectrum of a smaller field centered at the BEK observed with Chandra, and is scaled to the Micro-X field of view using the x-ray images obtained with the ROSAT X-ray Observatory.

4.1. Plasma Conditions and Shocked Clouds

The high quality of the Micro-X spectrum will provide a detailed look at the plasma conditions in Puppis A. Chandra observations indicate a rather complex temperature structure in the BEK region.[9] With 2 eV energy resolution, we will be able to diagnose the temperature structure in the x-ray emitting gas by identifying the Fe L lines that are present in the spectrum. Figure 8 shows a detail view of the Fe L region near 0.55–0.95 keV in the simulated spectrum, where lines of Fe XVII to Fe XIX are readily identified. The Fe L lines are powerful temperature diagnostics, as the relative emissivity curves of various Fe ions are different at different temperatures. The identification of the Fe ions and a measurement of their relative flux in the Micro-X spectrum will thus place direct constraints on the temperatures present in the plasma.

Supernova remnant plasmas are typically not in ionization equilibrium for their temperatures, because of their low densities. The supernova shocks (the two main ones being the forward shock associated with ambient material and the reverse shock associated with ejecta) heat the gas quickly, but the gas ionizes slowly by electron-ion collisions. The ionization structure is generally time-dependent throughout the lifetime of the x-ray emitting remnant. Diagnostics of nonequilibrium ionization are provided by the line intensity ratios of the resonance, forbidden, and intercombination triplet in He-like ions, as well as low ion species that may contribute a low-energy component to the main He-like blends and Fe XVI inner-shell transitions that may be visible near Fe XVII lines.

In addition to temperature and ionization information, another important diagnostic of the cloud-shock interactions will be given by the line profiles. A cloud that has encountered a shock will subsequently be torn

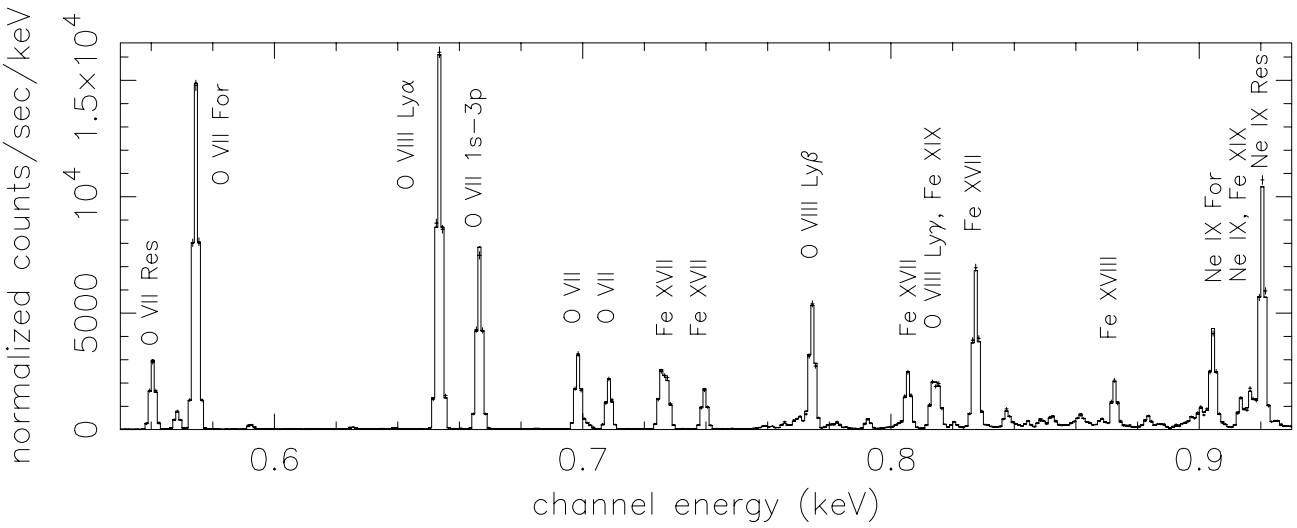

Figure 8. Detail of Puppis A simulated spectrum from Figure 7.

apart by hydrodynamic instabilities.[10] Chandra identified the inner region of the BEK to be a cloud that is in an advanced phase of this very process;[9] indeed it is the only identified astrophysical example of such a mature cloud-shock interaction to date. Line energy shifts and line widths will be imprinted by these turbulent processes. The Micro-X energy resolution and high signal to noise data will allow measurement of turbulent velocities down to ±10 km/s, which is the statistical resolution of our data, though systematic effects (due to calibration and gain uncertainties) may be a factor of 2 larger.

Because the BEK is a clump (or clumps) of interstellar material being overtaken by the shock, it is a promising region to find neutral material, and thus to observe the spectral signatures of charge exchange reactions. In its simplest form, astrophysical charge exchange (CEX) is the radiationless transfer of an electron from a neutral atom (usually H or He) to a highly charged ion, with subsequent emission of an x-ray photon as the transferred electron decays to the ground state. In the case of CEX between bare ions and neutral atoms, the high-n transitions are considerably stronger than in the case of collisional excitation,[11] resulting in anomalous Lyman series line intensity ratios. Such distinct spectral signatures make it possible to identify CEX and distinguish it from emission from a collisional equilibrium plasma, or one dominated by radiative recombination. The strength of the spectral signature can then be used to quantify the amount of neutral gas present, and the relative line intensities (in the case of CEX involving bare ions) used to determine the relative collision speed between the ions and neutrals.

Despite its large cross-section, the normally low abundance of neutral material generally prevents CEX from having a significant effect on the x-ray spectrum for supernova shocks in the sense of modifying the cooling power or total x-ray flux.[12] CEX would be enhanced, however, by turbulent mixing such as would occur when the shock interacts with a dense interstellar cloud as at the BEK. The general problem of how mixing occurs in a shock-cloud interaction is vital to understanding shock-induced star formation but is also difficult to model. Measurements (or limits) on the amount of CEX emission present in an actual shocked cloud would test such models in a new regime.[13]

4.2. Oxygen Enhancement

An enduring question surrounding Puppis A is the identification of x-ray emitting ejecta. Although the x-ray brightest features in the Puppis-A BEK have been identified as shocked interstellar clouds,[14] line strengths measured at high spectral resolution by the Einstein FPCS[7,8] indicated that, despite significant dilution by shocked ambient material, there is evidently an overall oxygen abundance enhancement arising from the presence of shocked oxygen ejecta synthesized by the remnant's massive progenitor.

Subsequent observations with CCD instruments having only moderate spectral resolution have not been able to definitively identify the oxygen ejecta, although observations with ASCA did indicate the presence of Ne ejecta in the western and southern regions of the remnant.[15] More recently, moderate spectral resolution observations with the Chandra ACIS instrument of the Bright Eastern Knot in Puppis A suggest that there is oxygen enhancement in localized regions near the shocked interstellar clouds.[9] It is not surprising that the ejecta should become highly fragmented and localized as the shock is interacting with a highly inhomogeneous environment. Tantalizingly, the optical ejecta knots are mostly contained within an angular distance of some ten arcminutes of the BEK. Line strengths measured directly relative to continuum in this region will unambiguously reveal the presence of ejecta, provided that the field of view captures an area enriched with ejecta and provided that we can be sure of the underlying temperature structure of the gas. The existing CCD spectra do not unambiguously indicate the temperature structure of the gas. We will tackle this problem by combining the analysis of the Micro-X data (which will have ~ 2.5 arcmin imaging) with ongoing and detailed analysis of data with better angular resolution (but poorer spectral resolution) from XMM-Newton, Chandra, and Suzaku. The high spectral resolution of the Micro-X spectrum will provide the crucial test of the underlying temperature structure of the gas and the measurement of line fluxes relative to the continuum to address the question of the presence of ejecta in Puppis A.

5. CONCLUSION

We are currently designing the payload for the Micro-X Rocket, and are on schedule for launch in early 2011. We have already begun to build some of the flight hardware for the mission, and most of the payload will be built and tested in the next year. This mission will launch the first TES microcalorimeter into space, will obtain a rich dataset from the Bright Eastern Knot region of the Puppis A supernova Remnant, will measure the plasma conditions and the ejecta/circumstellar material interactions, and will serve as a demonstrator of the technologies being developed for the Constellation-X mission.

REFERENCES

1. D. McCammon, R. Almy, E. Apodaca, W. Bergmann Tiest, W. Cui, S. Deiker, M. Galeazzi, M. Juda, A. Lesser, T. Mihara, J. P. Morgenthaler, W. T. Sanders, J. Zhang, E. Figueroa-Feliciano, R. L. Kelley, S. H. Moseley, R. F. Mushotzky, F. S. Porter, C. K. Stahle, and A. E. Szymkowiak, "A high spectral resolution observation of the soft x-ray diffuse background with thermal detectors," *ApJ* **576**, pp. 188–203, 2002.
2. F. S. Porter, R. Almy, E. Apodaca, E. Figueroa-Feliciano, M. Galeazzi, R. Kelley, D. McCammon, C. K. Stahle, A. E. Szymkowiak, and W. T. Sanders, "Observations of the soft X-ray background with the XQC microcalorimeter sounding rocket," *Nuclear Instruments and Methods in Physics Research A* **444**, pp. 175–179, 2000.
3. L. Duband, L. Hui, and A. Lange *Cryogenics* **33**, p. 643, 1992.
4. C. A. Kilbourne, S. R. Bandler, A.-D. Brown, J. A. Chervenak, E. Figueroa-Feliciano, F. Finkbeiner, N. Iyomoto, R. L. Kelley, F. S. Porter, and S. J. Smith, "Various Optimizations of TES Arrays for X-Ray Astrophysics," *Journal of Low Temperature Physics* **151**, pp. 223–228, Apr. 2008.
5. C. D. Reintsema, W. B. Doriese, F. S. Porter, R. G. Baker, and E. Figueroa-Feliciano *Proc. SPIE* **7011-80**, 2008.
6. E. Figueroa-Feliciano, S. R. Bandler, M. Bautz, K. Boyce, G. Brown, S. Deiker, W. B. Doriese, K. Flanagan, M. Galeazzi, G. C. Hilton, U. Hwang, K. D. Irwin, T. Kallman, R. L. Kelley, C. A. Kilbourne, S. Kissel, A. Levine, M. Loewenstein, D. Martinez-Galarce, D. McCammon, R. Mushotzky, R. Petre, F. S. Porter, C. D. Reistema, T. Saab, P. Serlemitsos, N. Schulz, R. Smith, and J. N. Ullom, "Science with Micro-X: the TES microcalorimeter x-ray imaging rocket," in *Space Telescopes and Instrmentation II: Ultraviolet to Gamma Ray*, M. J. L. Turner and G. Hasinger, eds., *Proceedings of the SPIE* **6266**, p. 62660A, July 2006.
7. K. A. Flanagan, "Plasma Diagnostics with X-Ray Emission Lines of Puppis A.," *MIT Ph.D. Thesis* , 1990.
8. C. R. Canizares and P. F. Winkler, "Evidence for elemental enrichment of Puppis A by a Type II supernova," *ApJL* **246**, pp. L33–L36, May 1981.

9. U. Hwang, K. A. Flanagan, and R. Petre, "Chandra X-Ray Observation of a Mature Cloud-Shock Interaction in the Bright Eastern Knot Region of Puppis A," *ApJ* **635**, pp. 355–364, Dec. 2005.
10. R. I. Klein, K. S. Budil, T. S. Perry, and D. R. Bach, "The Interaction of Supernova Remnants with Interstellar Clouds: Experiments on the Nova Laser," *ApJ* **583**, pp. 245–259, Jan. 2003.
11. P. Beiersdorfer, R. E. Olson, G. V. Brown, H. Chen, C. L. Harris, P. A. Neill, L. Schweikhard, S. B. Utter, and K. Widmann, "X-Ray Emission Following Low-Energy Charge Exchange Collisions of Highly Charged Ions," *Physical Review Letters* **85**, pp. 5090–5093, Dec. 2000.
12. M. W. Wise and C. L. Sarazin, "Charge transfer and X-ray emission from supernova remnants," *ApJ* **345**, pp. 384–392, Oct. 1989.
13. A. P. Rasmussen, E. Behar, S. M. Kahn, J. W. den Herder, and K. van der Heyden, "The X-ray spectrum of the supernova remnant 1E 0102.2-7219," *A&A* **365**, pp. L231–L236, Jan. 2001.
14. R. Petre, G. A. Kriss, P. F. Winkler, and C. R. Canizares, "A high-resolution X-ray image of Puppis A - Inhomogeneities in the interstellar medium," *ApJ* **258**, pp. 22–30, July 1982.
15. K. Tamura, "ASCA observation of the Puppis A supernova remnant," *Ph.D. Thesis* , 1994.